DMD2010-3878

AN ARTICULATING TOOL FOR ENDOSCOPIC SCREW DELIVERY

Joseph E. Petrzelka

Dimitris M. Chatzigeorgiou Manas C. Menon Michelle E. Lustrino Clara J. Stefanov-Wagner Alexander H. Slocum, Ph.D.

Massachusetts Institute of Technology Cambridge, Massachusetts, US

Suresh K. Agarwal, M.D.

Boston University Boston, MA, US

ABSTRACT

This paper describes the development of an articulating endoscopic screw driver that can be used to place screws in osteosynthetic plates during thoracoscopic surgery. The device is small enough to be used with a 12 mm trocar sleeve and transmits sufficient torque to fully secure bone screws. The articulating joint enables correct screw alignment at obtuse angles, up to 60° from the tool axis. A novel articulating joint is presented, wherein a flexible shaft both transmits torque and actuates the joint; antagonist force is provided by a super-elastic spring. Screws are secured against the driver blade during insertion and with a retention mechanism that can passively release the screw when it has been securely placed in the bone. The prototype has been fitted with a blade compatible with 2.0 and 2.3 mm self-drilling screws, though a different driver blade or drill bit can easily be attached. Efficacy of the tool is demonstrated by securing an osteosynthetic plate to a rib in a mock surgical setup. This tool enables minimally invasive, thoracoscopic rib fixation.

INTRODUCTION

An articulating tool for endoscopic placement of screws will enable minimally invasive internal fixation of rib fractures using video-assisted thoracic surgery (VATS). VATS is a well-established procedure for pulmonary resection, lung volume reduction, lung biopsy, and pericardial resection. By selectively ventilating one lung, much of the pleural cavity becomes accessible; an appropriate device for screw delivery enables VATS fixation of rib fractures using osteosynthetic plates.

Multiple fractures in adjacent ribs compromise thoracic stability and result in paradoxical motion (*flail chest*) during respiration. This condition is common; 4-10% of trauma patients have rib fractures, of which 10-15% exhibit paradoxical motion [1]. This condition is painful at best, but

also reduces respiratory efficacy; in extreme cases the fracture endangers the integrity of the lungs or heart. Chest wall instability can be treated by sedation of the patient or through artificial respiration, though internal fixation (placement of an osteosynthetic device) is often required. Nirula *et al.* [2] identify three cases in which fixation may be beneficial: (1) in the case of multiple fractures and paradoxical motion, (2) in the case of isolated fractures that result in significant pain, and (3) in the case of a previous fracture that has failed to heal. Engel *et al.* [1] describe a survey of literature demonstrated shorter ventilation times and ICU stays in *all cases* where internal fixation was used. Solberg *et al.* [3] report that internal fixation reduces ventilation time, ICU stay, and sepsis.

Despite the clear benefits of internal fixation, existing procedures are so invasive that many surgeons opt to treat

1 Reprinted with permission of Joseph E. Petrzelka, Dimitris M. Chatzigeorgiou, Manas C. Menon, Michelle E. Lustrino, Clara J. Stefanov-Wagner, Alexander H. Slocum, Suresh K. Agarwal

indications with ventilation and analgesia alone. Titanium osteosynthetic plates are perhaps the most prevalent fixation method in the literature; Nirula *et al.* [2] regard these as the standard against which other methods must compare. These plates are screwed to the anterior surface of the rib at each fracture site, requiring large incisions and separation of musculature. Acute Innovations recently introduced a U-plate design advertised as minimally invasive, though the device still requires a large incision, considerable dissection, and significant separation of musculature [4,5]. Literature in the field has called for further advances in minimally invasive procedures [2].

Performing internal rib fixation thoracoscopically would provide three distinct advantages. First, this approach eliminates the large incisions and separation of musculature required for existing techniques. Second, a mechanical advantage is obtained; a fracture constrained on the proximal surface will be placed in compression during normal respiratory stresses, offering greater stability and eliminating stress shielding. Third, the neurovascular bundle along the inferior edge of each rib is clearly visible during VATS placement such that the surgeon can avoid nerve contact and associated post-operative pain.

In this paper, we present a new articulating tool for delivery of self-drilling screws in a VATS procedure. We are aware of no prior art that accomplishes this result. The literature supports the use of ductile mandibular plates for fixation [1], a method preferred by the authors. In a VATS procedure, these plates can be delivered through small incisions using existing endoscopic tools. In this presentation, we focus exclusively on a novel device that can secure these plates using self-drilling bone screws.

The following sections will present the specific requirements for an endoscopic screw delivery device. Next, an overview of the device design is presented followed by engineering details of each component. A scale prototype is presented, and finally we demonstrate the efficacy of the device in a synthetic construct.

DEVICE REQUIREMENTS

Placement of osteosynthetic plates in a VATS procedure requires an articulating endoscopic driver to secure monocortical self-drilling screws. In this section, we discuss specific requirements for (1) an endoscopic device, (2) an articulating joint designed for the thoracic cavity, (3) a device for driving bone screws, and (4) a screw retention mechanism.

The end of the tool must be able to pass through a standard trocar sleeve at the site of incision. While a smaller trocar sleeve (and thus smaller tool) is clearly advantageous, we consider the case of a large 12 mm trocar sleeve. Hence, the tool must fit through a cylindrical opening 12 mm in diameter. Further, materials must be selected to be both (1) bio-inert and (2) resist high temperatures during autoclave sterilization.

The tool must articulate to allow placement of screws normal to the local surface of a curved rib. The end length of the tool (from the articulation joint to the tip of the driver) is directly related to the angle through which the same end must

articulate (Fig. 1). A shorter end length results in a smaller degree of articulation and improved maneuverability in the thorax, but a minimum length is imposed by the components that must be included. The minimum radius of curvature of the ribs imposes an upper limit on tool end length; from Mohr et al. [6] this is approximately 10 cm in adults. From the authors' surgical experience, 6 cm would result in a maneuverable tool. Assuming an end length of 6 cm, the tool end must articulate between neutral and 60°. The symmetry of the device allows this one direction of articulation to reach a partial hemisphere of screw orientations. From parametric modeling of rib geometry (data from [6]), 60° will allow full access to multiple anterior fractures through a single posterior incision. The articulation must have a resolution of at least 10° (the accuracy with which screws must be placed; [7]). This end length and level of articulation is comparable to those of conventional endoscopic staplers [11].

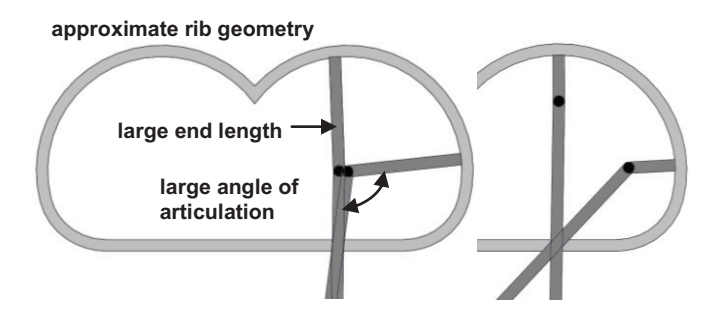


FIGURE 1 – AN ENDOSCOPIC DRIVER MUST HAVE AN ARTICULATING JOINT TO PLACE SCREWS AT THE CORRECT ORIENTATION; THE REQUIRED ANGLE OF ARTICULATION IS POSITIVELY CORRELATED WITH THE END LENGTH OF THE DEVICE. WHILE ILLUSTRATED HERE IN TWO DIMENSIONS, THE ADDITIONAL DEGREE OF FREEDOM ALLOWS ACCESS OF MULTIPLE FRACTURE SITES ON DIFFERENT RIBS THROUGH A SINGLE INCISION.

To start a screw into the rib cortex , a normal thrust force of 15 N must be exerted at the tip of the driver. Kincaid *et al.* [8] report starting loads on the order of 25 N for 3.5 mm self-tapping screws. Hillery and Shuaib [9] show thrust forces between 25 and 45 N for a 3.5 mm drill in cortical bone, depending on drill feed. In the authors' experience, self-drilling screws require very little thrust force to start driving (an order of magnitude less than the results reported here). Still, we obtain a conservative estimate by scaling the results in the literature for a 2.0 mm screw; this allows future adaptation of the device to drilling or self-tapping screw applications.

Hitchon *et al.* [10] find that the torque required to drive a 4 mm self-drilling screw in vertebrae is approximately 0.5 Nm, even at high bone mineral densities. Kincaid *et al.* [8] report similar values for 3.5 mm monocortical self-tapping screws in femurs. In comparison, drilling requires much less torque; Hillery and Shuaib [9] report values of 0.010 to 0.015 Nm for a 3.2 mm drill. Scaling these values linearly results in a torque requirement of approximately 0.25 Nm for a 2.0 mm screw. This scaling is quite conservative since the cortex of ribs is much thinner than that of constructs tested in the literature.

Finally, to avoid the loss of screws inside the body, the tool must actively retain the screw, at least on the order of magnitude of other forces (e.g. thrust force).

BACKGROUND

To the authors' knowledge, no device exists in prior art that satisfies the requirements set forth. While a variety of endoscopic tools are commercially available, few allow active tool articulation (e.g. Oberlin and Penrod [11], Nicholas *et al.* [12]) and none of these provide torque transmission.

Flexible shaft screw drivers are available for automotive and surgical use; patents by Prager and Volzow [13], Beyar and Sohn [14], and McGuire [15] use flexible shafts in surgical screw drivers, though their devices are either fixed-angle or unconstrained and thus unable to maintain a specific degree of articulation. Takehana *et al.* [16] use closed-loop control of shape memory alloy elements to direct the lens of a laparoscope, but their invention would be incapable of transmitting the high axial forces required for screw placement.

Devices for surgical screw placement commonly incorporate a screw holder of the type described by Stihl [17]; while this design is robust, it requires external actuation and is difficult to incorporate into an articulating device (Fig. 2). Schwager and Dorawa [18] describe another mechanical screw retention device, also requiring external actuation.

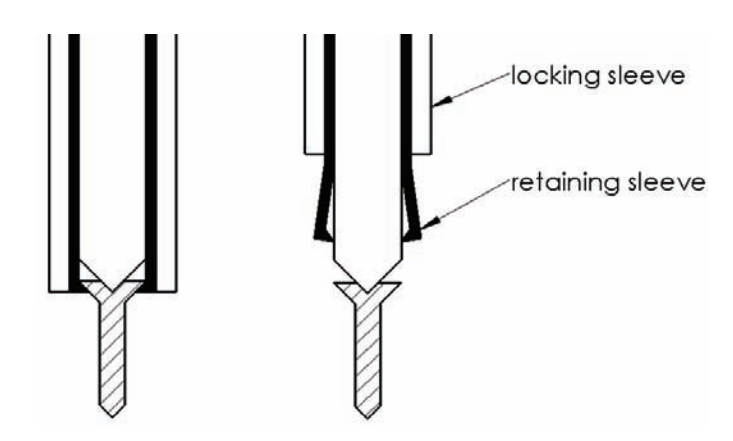


FIGURE 2 – COMMON SCREW RETAINER DESIGN; THE SCREW CAN BE EITHER HELD BY A SET OF RETAINING AND LOCKING SLEEVES (LEFT) OR RELEASED (RIGHT) [17].

We conclude that there are no existing mechanisms which accomplish the requirements of endoscopic screw placement.

DEVICE DESIGN

Our endoscopic screwdriver (Fig. 3) incorporates three degrees of freedom. Primarily, continuous (infinite) rotary motion must be provided at the tip of the screw. Second, an articulating joint must provide small angle rotations (0° to 60°). Third, a positive screw retention device must be actuated in a linear manner.

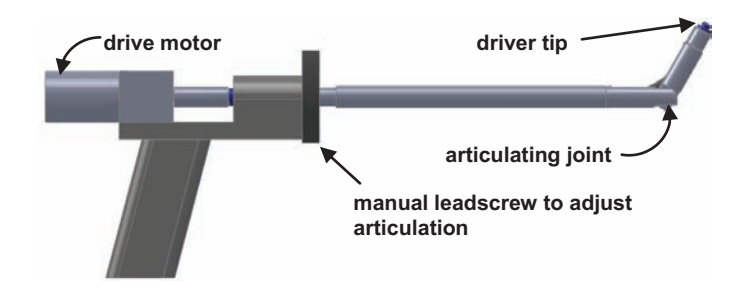


FIGURE 3 – ARTICULATING ENDOSCOPIC SCREW DRIVER, SHOWN AT MAXIMUM DEGREE OF ARTICULATION.

Rotary motion is provided via a flexible shaft that 'floats' through the articulating joint area. The joint pivots about two symmetric pins. Changing the arc length of the flexible shaft actuates the joint, with antagonist motion provided by a superelastic spring. While the flexible shaft runs along the axis of the device, the hinge pins are offset slightly to avoid a singularity at the neutral position. This arrangement is particularly desirable because it requires that only two components – the flexible shaft and the spring – pass through the hinge region. Further, the flexible shaft serves a dual role: it both transmits torque and controls articulation. This mechanism is illustrated in Fig. 4.



Figure 4 — Novel articulating joint design incorporating actuation via a torque-transmitting flexible shaft and antagonist actuation via a super-elastic spring (illustrated at the each extreme of articulation). A slot in the housing allows the flexible shaft to move off-center at high degrees of articulation.

A novel screw retention mechanism is located at the end of the shaft. This design uses an under-sized but compliant ring to hold the screw against the driver head; as the screw fully seats it pulls itself through the compliant ring to a released position. In this manner, the mechanism is passive and does not require external actuation (Fig. 5).

A drive module is connected to the articulating head via a tubular housing, through which a drive shaft passes. The drive module uses a DC motor to apply torque, though an alternative embodiment could allow manual or pneumatic power sources. A threaded nut changes the location of the housing with respect to the drive shaft, in effect changing the arc length of the flexible shaft and the angle of articulation (Fig. 6).

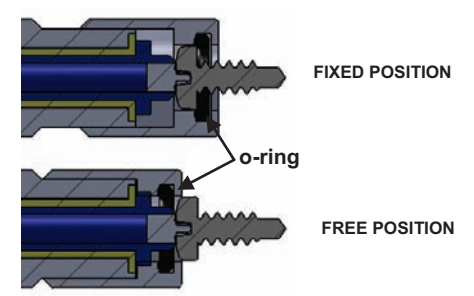


FIGURE 5 - NOVEL PASSIVE SCREW RETENTION MECHANISM DEMONSTRATING THE USE OF A COMPLIANT ELEMENT (O-RING) TO RETAIN THE SCREW TO THE DRIVER TIP; ILLUSTRATED IN BOTH THE FIXED AND FREE POSITIONS.

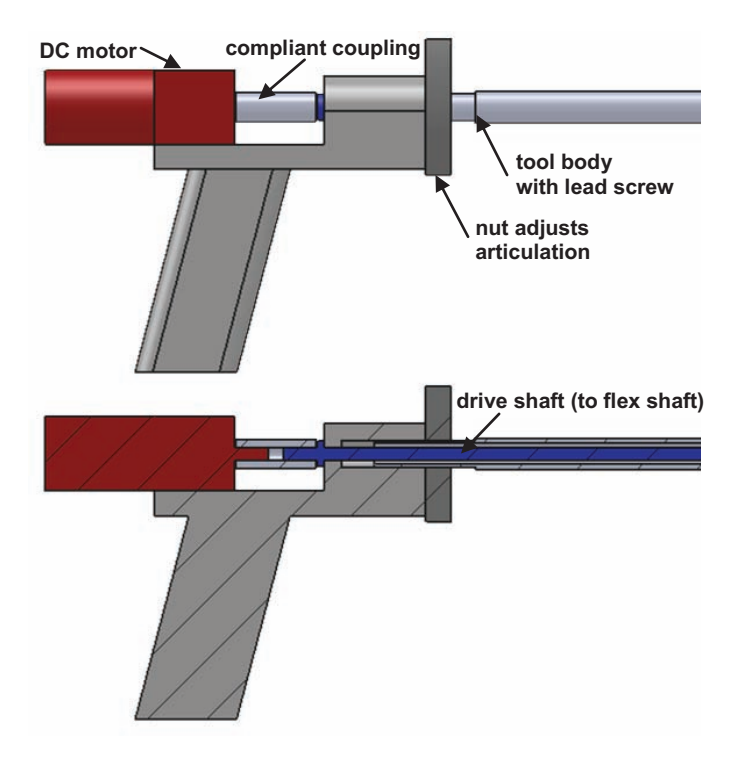


FIGURE 6 – EXTERNAL ACTUATION MECHANISM, INCORPORATING (1) A DC MOTOR FOR TORQUE AND (2) A LEAD SCREW TO ADJUST THE RELATIVE POSITION OF THE TOOL BODY AND DRIVE SHAFT (THUS CHANGING THE DEGREE OF ARTICULATION).

The following sub-sections discuss the specific mechanical element selection and engineering details for each module: torque transmission, joint actuation, screw retention, and surgeon control.

Torque Transmission

The primary function of the device is to drive a screw, requiring a transmission of torque. Further, this torque must be transmitted through a 60° variable-angle joint. From a survey of literature, we identify that 0.25 Nm should be sufficient to drive a 2.0 mm screw; however, we designed a device capable of providing 1.0 Nm, allowing for a generous safety factor. Further, the transmission element must consume only a fraction of the 12 mm envelope to allow fitting of other components (e.g. hinge and actuation elements).

Rigid mechanical elements are unable to transmit the required torque at the small scale desired. Variable-angle gear sets are

limited by both relative cost and size. A universal joint (U-joint) seems a natural choice for variable-angle torque transmission. The use of two serial U-joints results in constant velocity (impossible using a single U-joint) and requires each to flex only 30°. However, at the small diameters required, U-joints have detrimentally low torque ratings. A survey of commercially available stainless steel U-joints shows that a prohibitively large component would be required to achieve a reasonable design safety factor (Fig. 7).

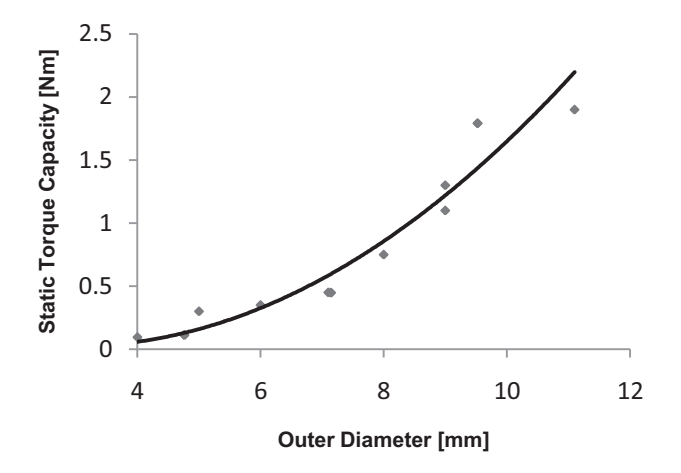


FIGURE 7 - STATIC TORQUE RATING VS. OUTER DIAMETER FOR STAINLESS STEEL UNIVERSAL JOINTS; CURVE SHOWS A BEST FIT TO DATA POINTS COLLECTED IN A SURVEY OF COMMERCIALLY AVAILABLE COMPONENTS.

A compliant element offers much higher torque transmission at small scales. Flexible shafts (flex shaft), wherein a cable core provides high torsional stiffness but low bending stiffness, offer an alternative to gear and U-joint systems. To our advantage, flex shafts are limited only by bend radius rather than absolute angle; thus, achieving a 60° bend is quite feasible. Further, flex shafts are capable of transmitting much higher torques than U-joints at the millimeter scale. The failure mode of a flex shaft is not shear, but rather helixing. The critical torque T_C at which the flex shaft becomes unstable is determined by its bending stiffness B, free length ℓ , and tension P [19]:

$$T_C = 2\sqrt{\frac{B^2\pi^2}{\ell^2} + BP} \tag{1}$$

Due to advantages of higher torque ratings at small size scales, this device uses a 3.3 mm flex shaft with a 50 mm bend radius and a 3.4 Nm maximum torque; testing shows that zero-tension helixing occurs at T_C of 1 Nm. The bend radius of this shaft dictates the required free length; from a geometric abstraction of the flex shaft (Fig. 8), one can show that

$$R = L \cot \frac{\theta}{2} - D \tag{2}$$

and thus determine the free length, $\ell=2L$, as a function of maximum angle of articulation θ and minimum bend radius R. Hence for our device a free length ℓ of about 60 mm is required (note that this only consumes half of the maximum end length of 6 cm, leaving room for bushings and a driver

blade). Further, the distance that the shaft moves from neutral is

$$d = L \left[1 - \cos \frac{\theta}{2} \right] / \left[\sin \frac{\theta}{2} \right] \tag{3}$$

In the present embodiment, this results in a deflection d of 8 mm, requiring that a channel be provided such that the shaft can flex a small distance outside the tool housing at full articulation. At a neutral position (zero degrees articulation) the shaft is fully within the tool housing for movement through the trocar sleeve (Fig. 4).

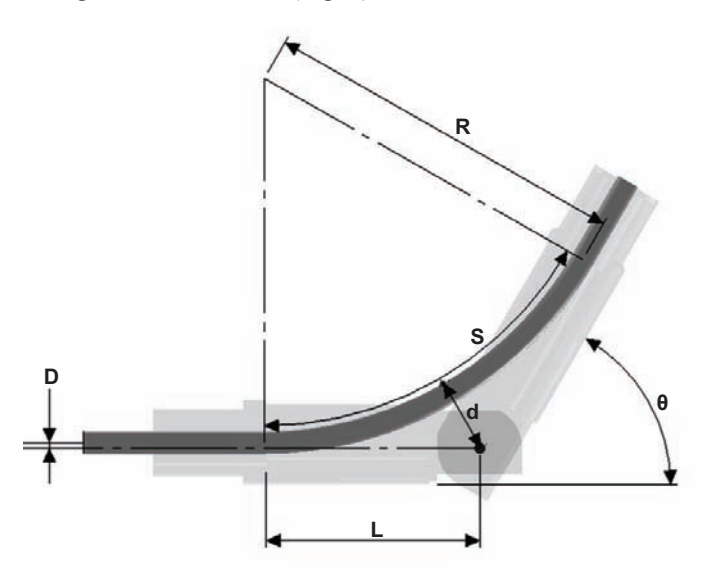


Figure 8 – Model of flexible shaft geometry as a function of articulation angle θ , pivot length L, and pivot offset D.

Joint Actuation

As a secondary function, the device must articulate between zero and sixty degrees; the mechanism of actuation is not a trivial design problem given the size constraints and anticipated forces. A four-bar linkage would allow fully actuated control of the articulation angle, but at this small scale link buckling and pin shear become problematic. To solve these problems, we developed an under-actuated design that utilizes a tensile element coupled with an antagonist spring.

The flexible shaft acts as the tensile element necessary to actuate the joint. Based on Eqn. 2 and Fig. 8, the arc length of the flexible shaft is a function of articulation angle θ :

$$S = \theta \left[L \cot \frac{\theta}{2} + D \right] \tag{4}$$

Alternatively, the articulation angle can be expressed as a function of shaft arc length, thus allowing a deterministic change of articulation angle by modifying the relative position of the tool housing and flexible shaft. This relationship can be observed in Fig. 9; note the different locations of the flexible shaft driven end at the extremes of articulation. To avoid a singularity at $\theta=0$, the pivot point of the joint is placed slightly above the centerline of the flexible shaft (distance D in Fig. 8).

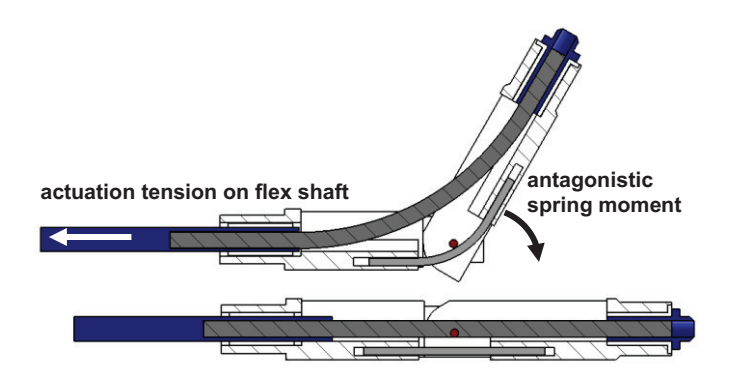


FIGURE 9 — SCHEMATIC ILLUSTRATING THE CHANGE IN FLEX SHAFT ARC LENGTH BETWEEN THE EXTREMES OF ARTICULATION; ACTUATION TENSION IN THE FLEX SHAFT IS BALANCED BY AN ANTAGONISTIC BEAM SPRING.

The size constraints of this device motivate selection of a super-elastic nitinol (NiTi) antagonist spring. An ideal antagonist device would provide a force of the same magnitude as the thrust force (15 N) along the entire range of articulation. Constant force springs made from standard materials (i.e. spring steels) are too weak at the scale required. The force exerted by a cantilevered beam spring configuration is governed by beam bending theory and is proportional to the curvature, ρ , and radius, r, which are related to the yield strain according to

$$r = \varepsilon_{\text{yield}} / \rho_{\text{max}} \tag{5}$$

The curvature ρ_{max} is dictated by design geometry (similar to Eqn. 2); hence this configuration results in an extremely small spring diameter and low forces for conventional materials. However, the super-elastic properties of NiTi provide a yield strain (ε_{yield}) that is an order of magnitude greater than conventional materials, while maintaining a relatively constant stress level $(\sigma_{superelastic})$. Thus, the use of a NiTi beam spring allows a constant, yet significant, antagonist force in a small envelope (Fig. 10).

Hard stops are incorporated in the housing design at each extreme to prevent over-articulation of the joint in this under-actuated configuration.

To validate this design, each structural force and tension were computed as a function of articulation angle θ . These calculations show that the shear force on the pin joint, the flexible shaft tension, and the actuation force are nearly identical (Fig. 11). Each of these forces are well below the yield point of their respective mechanical elements.

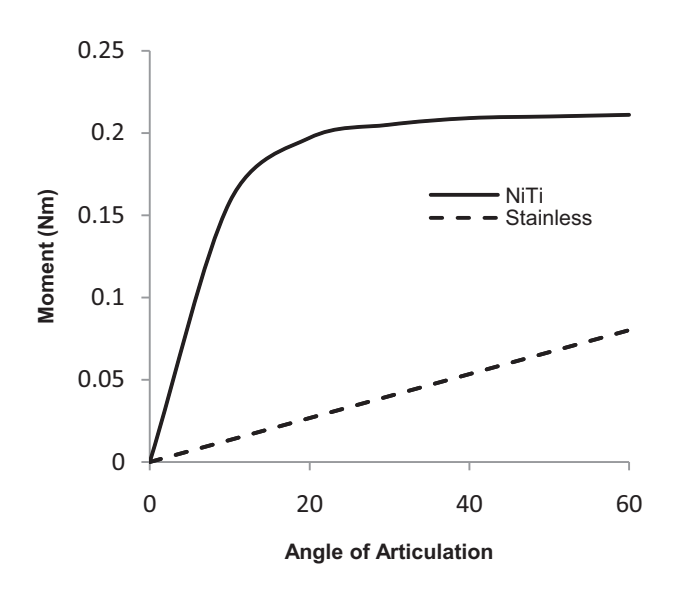


Figure 10 – Graph of antagonist moment (Nm) as a function of articulation angle for NiTi and stainless steel beam springs at a maximum curvature of $72~\text{m}^{-1}$. The super-elastic NiTi provides a larger and more uniform antagonistic moment.

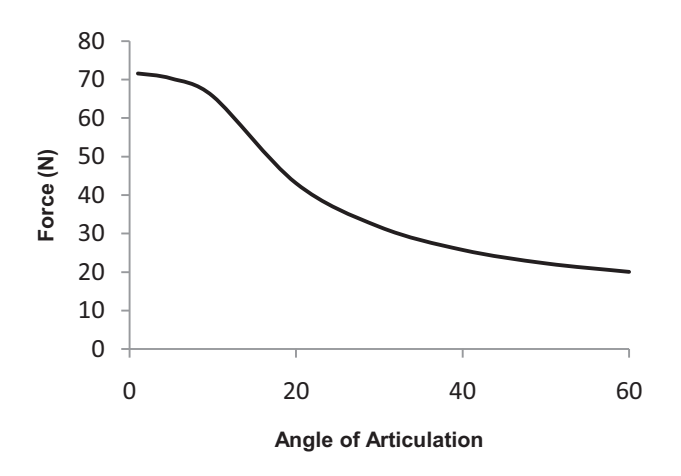


FIGURE 11 – GRAPH OF FLEX SHAFT TENSION (N) AS A FUNCTION OF ARTICULATION ANGLE; PIN SHEAR FORCE AND ACTUATION FORCE ARE OF SIMILAR MAGNITUDE AND RESPONSE.

Screw Retention

While a variety of screw retention devices exist in current art, each requires actuation of some variety. Due to the limited space available in the articulating joint, a passive device is preferred. To this end, a sliding sleeve is installed at the driver tip of the device. This sliding sleeve incorporates a compliant element (o-ring) that acts to retain the screw against the driver tip. When axial loading between the screwdriver and the rib surface reaches a critical threshold (order of 10 N), the screw slips through the compliant ring (Fig. 12). Reasonable radial forces (of order 10 N) fail to dislodge the screw from this retention device, thus ensuring that the screw will not fall off inadvertently during surgery.

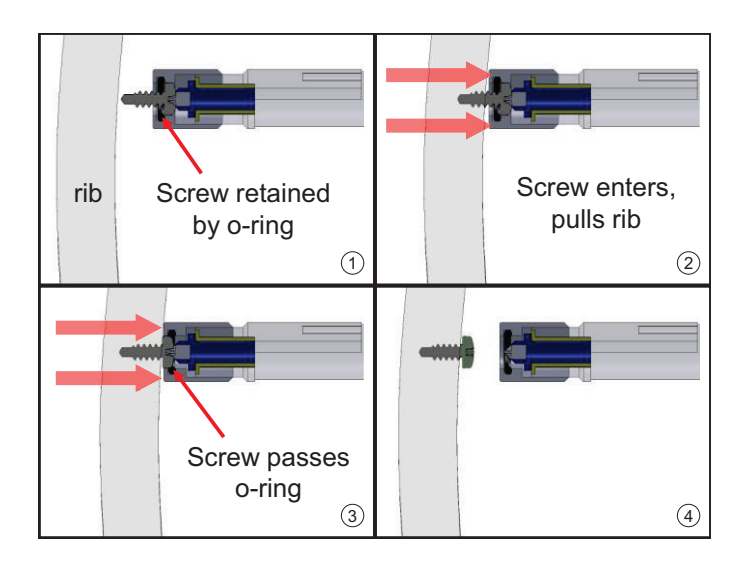


FIGURE 12 – SCHEMATIC OF THE NOVEL PASSIVE SCREW RETAINER: THE SCREW IS FIRMLY HELD BY THE RETAINER DURING DEVICE INSERTION (1) AND SCREW INSERTION (2), BUT IS ALLOWED TO PASS THROUGH THE COMPLIANT O-RING AS IT FULLY SEATS INTO THE RIB OR OTHER CONSTRUCT (3). FINALLY, THE SECURE SCREW IS FREED FROM THE DRIVER TIP (4).

Surgeon Control

A handle is incorporated to allow device control outside the body. This grip must provide a means of (1) applying torque and (2) actuating the wrist.

Torque can be applied via a number of equally acceptable methods, including manual, electric, or pneumatic drives. Any powered drive must have a peak torque on the order of 1 Nm, be able to operate at about 60 RPM with variable speed control. In this embodiment, we chose a DC gear motor for cost and ease of control. By applying variable voltage, the torque and speed can be controlled relatively well. Ideally, high gain velocity feedback would allow more precise control. The motor is mounted at the rear of the handle, using a flexible coupling to eliminate axial loading and mitigate alignment errors (Fig. 13).

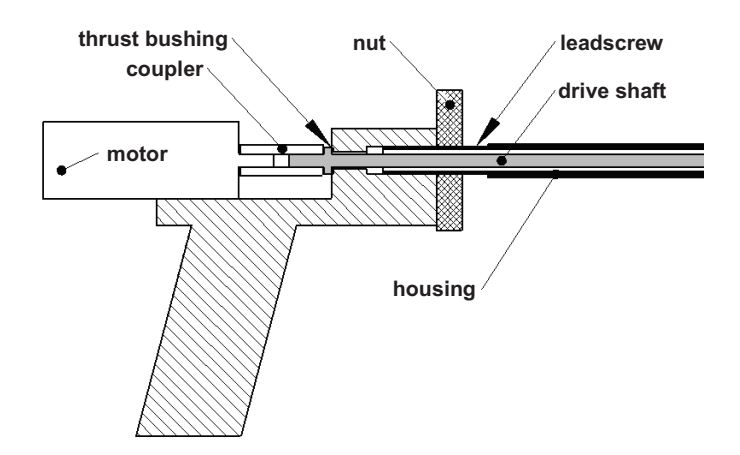


FIGURE 13-GRIP DESIGN: DRIVE MOTOR PROVIDES TORQUE TO THE DRIVESHAFT THROUGH A COUPLING; LEADSCREW ADJUSTS RELATIVE POSITION OF THE DRIVE SHAFT AND HOUSING TO CONTROL ARTICULATION.

Articulation is controlled by changing the relative position of the drive shaft (coupled to the flex shaft) and the main housing; this is accomplished by turning of a nut located near the handle of the tool. The total movement required follows from the change in arc length (Eqn. 4):

$$\Delta S = 2L - \theta \left[L \cot \frac{\theta}{2} + D \right] \tag{6}$$

In the present design, ΔS of 6 mm is required for articulation of 60°. While a number of mechanisms could accomplish this, a nut / leadscrew combination is chosen for fine resolution and stability (assuming it cannot be backdriven). The drive shaft is retained against a bushing so that its axial load is decoupled from the drive motor. Feedback is provided either through visual inspection of the articulating end or by incorporating a rule into the grip that correlates ΔS with θ .

PROTOTYPE / TESTING

Prototypes were constructed and tested. A surgical simulation, complete with trocar sleeve, self-drilling bone screws, and osteosynthetic plates, was used to test the driver. The screw retention device was prototyped and tested independently. Results from a swine cadaver trial are forthcoming.

Articulating Driver

The novel articulating elbow and preferred grip embodiment were prototyped for testing. Each housing at the articulating joint was machined from 7075 aluminum; the majority of other internal components were manufactured from various stainless steel alloys (e.g. flex shaft, drive shaft, pivot pins, primary housing). Rulon bushings were used at each end of the flex shaft for biocompatibility and autoclave temperature resistance. The handle was constructed from inexpensive 6061 aluminum tubing, nylon bushings, and ABS plastic. A custom knurled nut was machined for articulation control. A driver blade was machined at the end of the flex shaft, similar to Stryker part 60-20140. The entire device weighs 660 g (Fig. 14).

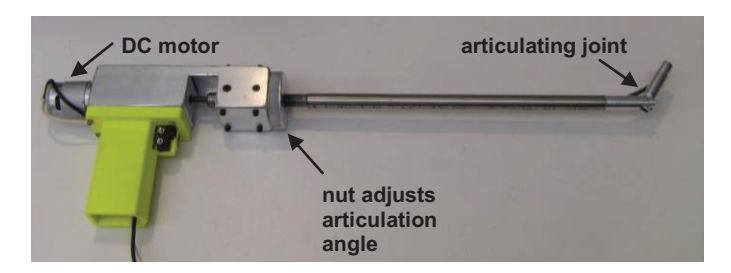


Figure 14 – A prototype of the endoscopic driver: the articulating joint is actuated by the flex shaft, while the remote handle incorporates a DC gear motor and separate lead screw for adjusting articulation. The entire device weighs $0.66~{\rm kg}$.

The end of the tool easily fits through a 12 mm trocar. The angle of articulation can be adjusted evenly between 0° and 60° by turning the leadscrew nut (Fig. 15). The total end length of the device is approximately 5 cm from the articulating joint to the driver tip.

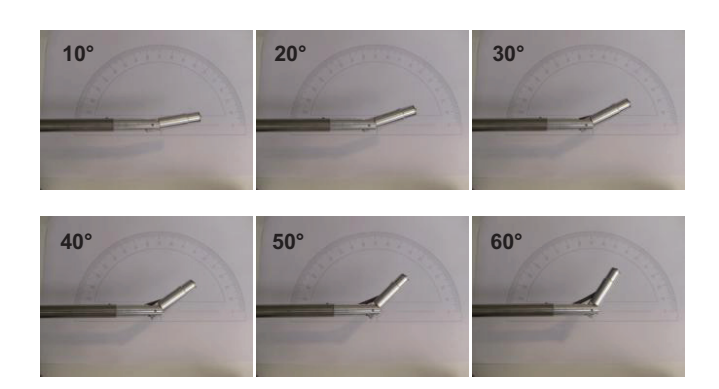


Figure 15 – The tool successfully articulates from 0° (neutral) to 60° with continuous resolution; angles of 10° through 60° are illustrated here.

A surgical simulation was constructed using a mock plastic trocar sleeve and a swine rib placed at realistic positions (Fig. 16). Six-millimeter self-drilling bone screws (Stryker part 50-20906) were successfully driven into the rib cortex. To demonstrate the feasibility of VATS rib fixation, a malleable craniomaxillofacial reconstruction plate was secured to the rib in the mock setup (Fig. 17).



FIGURE 16 - MOCK SETUP, INCLUDING TROCAR SLEEVE AND RIB, USED TO TEST THE ENDOSCOPIC DRIVER PROTOTYPE. THE TROCAR SLEEVE IS SIMULATED BY A SIMPLE PLASTIC TUBE AND THE RIB IS FIXED IN A VICE.



FIGURE 17 – OSTEOSYNTHETIC PLATE SUCCESSFULLY SECURED TO RIB USING SELF-DRILLING SCREWS AND THE PROTOTYPE ENDOSCOPIC DRIVER

Screw Retainer

An aluminum sleeve was machined and assembled with an oring to test the efficacy of the retainer design. Using #6 self-drilling screws, a #1 Phillips driver, and a 1/4 inch by 3/8 inch oring, an axial force of about 25 N was required to remove

the screw from the driver. The screw could not be dislodged from the retainer with reasonable radial forces. The passive action of the device was verified in a synthetic (maple) construct (Fig. 18).

For surgical use, a Kalrez o-ring would be both biocompatible and resistant to autoclave temperatures. The sleeve could be made from a polymer, anodized aluminum, or stainless steel.



FIGURE 18 - THE SCREW RETAINER MODULE IN ACTION

CONCLUSION / FUTURE WORK

We present a new device for endoscopic screw placement. This tool enables a new paradigm for internal fixation of rib fractures, using well established VATS procedures. Using a novel articulating joint, the device can place screws at obtuse angles (up to 60° off-axis) to meet the local curvature of ribs while delivering relatively high levels of torque. The device can easily be adapted to other surgical applications by attaching different driver trips or drill bits.

A scale prototype proves design feasibility. Testing in a mock setup demonstrated promising results for VATS fracture stabilization.

Our future endeavors include a swine cadaver study and further development of this device for commercialization.

ACKNOWLEDGEMENTS

This device was developed as a term project in MIT Course 2.75: Precision Machine Design. We are grateful to Lynn Osborn and Dr. Tom Brady of *The Center for Integration of Medicine and Innovative Technology* (www.cimit.org) for providing support for Course 2.75 and this project (DOD funds, FAR 52.227-11). We are also grateful to the Boston University School of Medicine, Dave Custer, Conor Walsh, and Nevan Hanumara for their support and guidance throughout the project. Finally, we thank SolidWorks Corporation for providing solid modeling software.

REFERENCES

- [1] Engel, C., Krieg, J.C., Madey, S.M., Long, W.B., and Bottlang, M., 2005, "Operative Chest Wall Fixation with Osteosynthesis Plates," *Journal of Trauma*, 58(1), pp. 181-186.
- [2] Nirula, R., Diaz, J.J., Trunkey, D.D., and Mayberry, J.C., 2009, "Rib Fracture Repair: Indications, Technical Issues, and Future Directions," *World Journal of Surgery*, 33(1), pp. 14-22.
- [3] Solberg, Moon, Nissim, Wilson, and Marqulies, 2009, "Treatment of Chest Wall Implosion Injuries without Thoracotomy: Technique and Clinical Outcomes," *Journal of Trauma*, 67(1), pp. 8-13.

- [4] *RibLoc*, 2009, Accute Innovations, < http://www.acuteinnovations.com/Products/RibLoc >, accessed November 2009.
- [5] Sales, Ellis, Gillard, Liu, Chen, Ham, and Mayberry, 2008, "Biomechanical Testing of a Novel, Minimally Invasive Rib Fracture Plating System," *Journal of Trauma*, 65(5), pp. 1270-4.
- [6] Mohr, M., Abrams, E., Engel, C., Long, W.B., and Bottlang, M., 2007, "Geometry of Human Ribs Pertinent to Orthopedic Chest-Wall Reconstruction," *Journal of Biomechanics*, 40, pp. 1310-17.
- [7] Wolter, D., 2001, Fixation System for Bones, US 6,322,562.
- [8] Kincaid, B., Schroder, L., and Mason, J., 2007, "Measurement of Orthopedic Cortical Bone Screw Insertion Performance in Cadaver Bone and Model Materials," *Experimental Mechanics*, 47, pp. 595-607.
- [9] Hillery, M.T., and Shuaib, I., 1999, "Temperature Effects in the Drilling of Human and Bovine Bone," *Journal of Materials Processing Technology*, 92, pp. 302-8.
- [10] Hitchon, P.W., Brenton, M.D., Coppes, J.K., From, A.M., and Torner, J.C., 2003, "Factors Affecting the Pullout Strength of Self-Drilling and Self-Tapping Anterior Cervical Screws," *Spine*, 28(1), pp. 9-13.
- [11] Oberlin, J.R., and Penrod, M.A., 1998, Articulated Surgical Instrument with Improved Articulation Control Mechanism, US 5,725,536.
- [12] Nicholas, D.A., Russell, B.G., Zvenyatsky, B., Matula, P.A., and Remiszewski, S.H., 1996, *Articulating Endoscopic Surgical Apparatus*, US 5,490,819.
- [13] Prager, R. and Volzow, S., 2008, Screwdriver for Bone Screws, US 2008/0243436 A1.
- [14] Beyar, M. and Sohn, Z., 2003, System for Bone Screw Insertion, US 6,663,642 B2.
- [15] McGuire, D.A., 1995, Flexible Surgical Screwdriver and Methods of Arthroscopic Ligament Reconstruction, US 5,464,407.
- [16] Takehana, S., Ueda, Y., Gotanda, M., Sakurai, T., and Adachi, H., 1990, *Apparatus for Bending an Insertion Section of an Endoscope Using a Shape Memory Alloy*, US 4,930,494.
- [17] Stihl, E., 2001, Screwdriver, US 6,189,422 B1.
- [18] Schwager, M. and Dorawa, K., 2008, *Bone Screw Holding Device*, US 2008/0269768 A1.
- [19] Black, A. Robert, 1988, "On the Mechanics of Flexible Shafts," *PhD Thesis, Stevens Institute of Technology*.